IEEE Access
Multidisciplinary ⋮ Rapid Review ⋮ Open Access Journal

Received 5 September 2026, accepted 23 September 2026, date of publication 2 October 2026, date of current version 12 October 2026.

*Digital Object Identifier 10.1109/ACCESS.2026.3739478*

RESEARCH ARTICLE

# Analysis of the Effect of Coil Shape and Size on AC Copper Loss in Slotless PMSM

**HYEONBIN HONG, HEEWON KOO, CHAEWON JO, CHANWOO SON, AND JU LEE, (Senior Member, IEEE)**
Department of Electrical Engineering, Hanyang University, Seoul 04763, Republic of Korea
Corresponding author: Ju Lee (Julee@hanyang.ac.kr)

This work was supported by Korea Planning and Evaluation Institute of Industrial Technology (KEIT), Republic of Korea, under Grant RS-2024-00507566.

**ABSTRACT** This paper investigates the mechanisms of alternating current (AC) copper losses in slotless permanent magnet synchronous motors (PMSMs) and analyzes the impacts of coil shapes and dimensions on AC copper losses and motor efficiency using finite element analysis (FEA). Slotless PMSMs offer distinct advantages, such as the elimination of cogging torque and its associated torque ripple owing to the absence of stator core slots, making them highly suitable for high-precision control and high-speed operation. However, it should be noted that torque ripple caused by back-EMF or current harmonics can still remain. However, because there is no stator core, the time-varying magnetic flux generated by the rotating permanent magnets directly links with the copper coils, significantly increasing AC copper losses due to the proximity effect. In this study, the effects of DC copper loss and AC copper loss are separated and thoroughly analyzed as the diameter and width of round and square coils are varied, while the stack length is adjusted to maintain the same output power specification. The analysis reveals that for round coils, a specific diameter balances the DC and AC copper losses, yielding the maximum efficiency. Furthermore, for square coils, minimizing the coil width ($l_x$) perpendicular to the permanent magnet flux is an effective design approach to reduce AC copper losses and maximize motor efficiency. These findings demonstrate that optimizing coil specifications is critical for mitigating AC copper losses when designing high-speed, high-precision slotless PMSMs. The novelty of this work lies in decomposing the AC copper loss into a current-induced (armature-reaction) component and a component produced by the direct linkage of the permanent-magnet flux, revealing that the proximity loss due to the permanent-magnet flux is dominant in slotless PMSMs; the output is then compared for round and square coil shapes through the trade-off relationship between the DC and AC copper losses under the same slot area and output constraints. In addition, a novel block-type coil stator that circumvents existing slotless-winding patents is proposed and the overall motor performance incorporating AC copper loss effects is experimentally validated.

**INDEX TERMS** AC copper loss, coil shape, coil size, finite element analysis(FEA), permanent magnet synchronous motors(PMSMs), proximity effect, skin effect, slotless motor.

## I. INTRODUCTION

Permanent magnet synchronous motors (PMSMs) are widely used in applications such as electric vehicles, home appliances, robotics, and servo systems because they can achieve higher torque density than conventional induction motors. Generally, PMSMs are divided into two types: slotted and slotless. Slotted PMSMs have a higher torque density than slotless ones, making them more popular in many applications [1]. However, slotted PMSMs suffer from cogging torque due to magnetic alignment between the permanent magnets and the stator core slots. In addition, slot openings generate spatial harmonics, increasing torque ripple and eddy-current losses in the permanent magnets,

The associate editor coordinating the review of this manuscript and approving it for publication was Jinquan Xu.

© 2026 The Authors. This work is licensed under a Creative Commons Attribution 4.0 License.
For more information, see https://creativecommons.org/licenses/by/4.0/

which eventually lead to motor vibration and noise. These problems make it difficult to use slotted PMSMs in high-precision fields. In contrast, slotless PMSMs do not have a slotted stator structure, so they are largely free from cogging torque and permanent-magnet eddy-current losses. However, torque ripple caused by back-EMF or current harmonics can still be present. Therefore, they are very useful in specific applications such as precision control and high-speed operation [2]. Because of these advantages, many studies have been conducted on PMSMs in various fields. Most of these studies focus on improving output performance through optimal motor design. However, there is still a lack of research on AC copper losses, which have recently caused many problems in PMSMs. In particular, slotless PMSMs are highly affected by AC copper losses because they lack a stator core, yet research on this is still insufficient compared to that on slotted PMSMs. In [3], to reduce AC copper losses in a slotless PMSM for a flywheel energy storage system (FESS), the authors analyzed the effects of coil diameter, current, and rotational speed, finding that coil diameter has a major impact on AC copper losses. They proposed a parallel winding structure. In [4], an analytical model was developed to predict AC copper losses over a range of 0-200 [Hz] with a maximum error of 5% or less compared to 2D finite element method (FEM) results. In [5], a method was investigated to accurately predict temperature-dependent AC and DC copper losses in PMSMs. In [6], a small slotless permanent-magnet motor was designed with distributed hexagonal windings. In [7], a method for accurately predicting proximity losses, a type of AC copper loss, in square conductors was discussed. In [8], a new model was developed to quickly calculate AC copper losses in an axial-flux motor with square coils, avoiding the time-consuming 3D FEM. In [9], the proximity effect losses in permanent magnet motors were analyzed, and loss-reduction methods based on conductor shapes were studied. In [10], the effect of eccentricity on AC copper losses in high-speed slotless permanent magnet motors was investigated. In [11], because circulating currents caused by inductance imbalance in parallel circuits increase AC copper losses in PMSMs, a method to reduce these currents was studied. In [12], a method to reduce AC copper losses by applying a magnetic plating coating to the copper coils used in permanent magnet motors was investigated. In [13], the effect of winding connection methods on AC copper losses in PMSMs was studied. In [14], the effects of coil shapes and power-source types on AC copper losses in high-speed PMSMs were analyzed. In addition, many studies have been conducted to improve the output characteristics of PMSMs. In [15], the electromagnetic performance of slotted and slotless axial flux motors was analyzed for aerospace or industrial compressor systems. In [16], the electromagnetic loss characteristics of slotted and slotless PMSMs were analyzed as a function of speed. In [17], a high-power design study was conducted for a slotless synchronous motor with a litz coil and a Halbach array. In [18], the output characteristics of PMSMs were analyzed as a function of sleeve thickness and material. In [19], the effects of various types of eccentricity on the electromagnetic characteristics of slotless PMSMs were investigated. In [20], considering the inherently low inductance of high-speed slotless PMSMs, the effects of current harmonics, torque ripple, and voltage distortion were studied. In [21], a new design method for slotless PMSMs was investigated by using printed circuit boards (PCBs) instead of conventional coils. In [22], the average torque and torque ripple of an axial flux motor were calculated using the Maxwell stress tensor method and verified by comparing them with 3D FEM and experimental results. In [23], a study was conducted to reduce vibration in a slotless moving-armature motor by altering the armature coil's motion. In addition, beyond loss analysis, extensive research has addressed the comprehensive optimization of PMSM efficiency and electromagnetic performance using different multi-objective optimization methods. In [24], the motor performance was optimized by adopting a surrogate model together with a multi-objective optimization algorithm based on NSGA-III. In [25], an improved sequential Taguchi method was introduced into motor optimization. In [26], transfer learning was applied to reduce the heavy computational cost caused by finite-element simulation. These works focus on overall electromagnetic performance optimization; however, the AC copper loss mechanism specific to slotless structures which must be understood prior to such optimization remains insufficiently studied. The present work is complementary to these studies: rather than optimizing global performance, it focuses on clarifying the AC copper loss mechanism that is intrinsic to slotless PMSMs and must be understood before such design optimization can be applied. As mentioned above, various studies have been conducted on PMSMs. However, studies focusing specifically on AC copper losses in slotless PMSMs are still insufficient. Therefore, this paper investigates the mechanisms of AC copper losses in slotless PMSMs and analyzes them as a function of coil shape, coil size, and housing configurations, thereby confirming their importance.

In this study, rather than focusing on the optimization of slotless PMSMs, the AC copper loss phenomenon, which is essential to the optimal design of slotless PMSMs, is analyzed. Using finite element analysis, the AC copper loss is separated into a component due to armature reaction and a component due to the proximity effect of the permanent-magnet flux, and it is confirmed that the proximity effect caused by the permanent magnets is dominant in the AC copper loss. When the slot area and the output are kept constant, the variation in output is analyzed through the trade-off relationship between the AC and DC copper losses arising from the changes in the number of turns and the stack length according to the coil size and shape, and the AC copper loss is further analyzed according to the presence and thickness of the housing. In addition, for a slotless PMSM whose development had been restricted by existing exclusive patents, a new block-structured winding method is proposed, a prototype

is fabricated, and the analysis results are verified through testing.

## II. AC COPPER LOSS MECHANISM OF SLOTLESS MOTOR

### A. ELECTROMAGNETIC LOSS

Electromagnetic losses in permanent magnet synchronous motors (PMSMs) include copper losses, core losses, and PM eddy-current losses. However, since this paper focuses on slotless PMSMs, PM eddy loss and rotor core loss are very small and can be neglected. This is because slotless PMSMs lack slot openings, unlike slotted PMSMs, so there are no spatial harmonics due to permanent magnet rotation. Therefore, PM eddy loss and rotor core loss are small enough to be ignored. Consequently, copper loss and core loss in slotless PMSMs can be expressed as follows [27].

$$P_{copper} = \frac{N_s N_{ph}^2 \left(L_{stk} + L_{end}\right)}{m\sigma K_{sf} a^2 A_{slot}} I_{rms}^2 \tag{1}$$

$$P_{core} = \int_{iron} \sum_{n} \left[k_h \left(nf\right) B_n^2 + k_e \left(nf\right)^2 B_n^2\right] \left(1 + \lambda C_n\right) \rho_c dv \tag{2}$$

where, $P_{copper}$ is the copper loss, $N_s$ is the number of slot, $N_{ph}$ is total series turn, $L_{stk}$ is Stack length, $L_{end}$ is the end length of winding, $\sigma$ is the conductivity of copper, $K_{sf}$ is the slot fill factor, $a$ is the number of parallel branch, $A_{slot}$ is the area of slot, $I_{rms}$ is the rms value of current, $P_{core}$ is core loss, $k_h$ and $k_e$ are adaptive hysteresis and eddy-current loss coefficients, $\rho_c$ is the density of core, $f$ is the electrical frequency, $B_n$ and $C_n$ are amplitude of flux density and short axis to long axis rate of the flux vector locus at harmonic order $n$, and $\lambda$ is the weight factor.

### B. SKIN EFFECT

AC copper losses in permanent magnet synchronous motors (PMSMs) are due to the skin effect and proximity effect. As shown in Fig. 1, (a) when an AC current flows through a copper coil, a time-varying magnetic field is generated around the current according to Ampere's law. This changing magnetic field induces eddy currents in the coil, according to Faraday's law of induction, in a direction that opposes the main current flow. Because these eddy currents flow in the opposite direction to the main current at the center of the coil, the current cannot flow through the center. On the other hand, at the surface, the eddy currents flow in the same direction as the main current, facilitating its flow. As a result, almost no current flows through the center of the copper coil, and most of it flows near the surface. This reduces the effective cross-sectional area and increases the effective resistance, thereby increasing copper losses; this phenomenon is called the skin effect. The skin effect can be expressed as shown in (3), which indicates that the skin depth decreases as the frequency increases or when a material with higher conductivity is used. In other words, if a large-diameter copper coil is used in a high-speed motor operating at a high

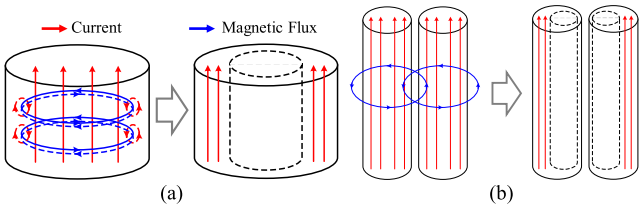



**FIGURE 1.** Types of AC copper loss (a) Skin effect, (b) Proximity effect.

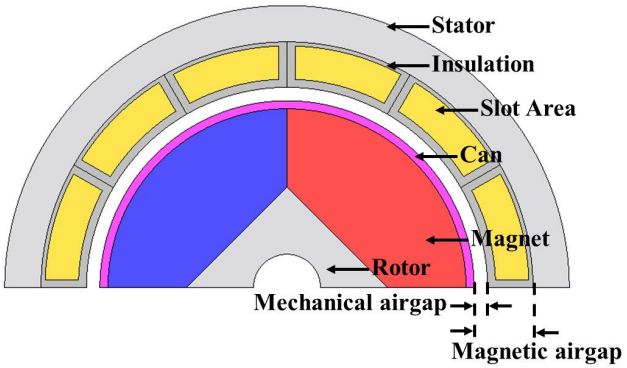



**FIGURE 2.** Geometry of slotless PMSM.

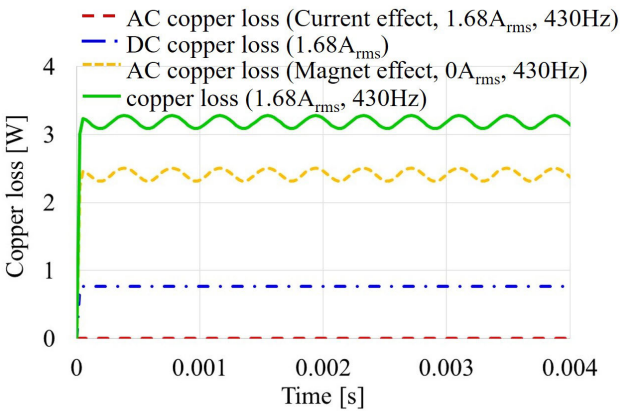



**FIGURE 3.** DC and AC copper loss separation in slotless PMSM at coil diameter 0.8[mm].

frequency, the main current flows only on the coil's surface due to the skin effect, thereby significantly increasing copper losses. Therefore, a smaller-diameter copper coil should be used [14], [16], [28], [29].

$$\delta = \sqrt{\frac{2}{\omega\mu\sigma}} = \sqrt{\frac{1}{\pi f \mu\sigma}} \tag{3}$$

where $\omega$ is the angular frequency, $f$ is the frequency, $\mu$ is the magnetic permeability of the material, and $\sigma$ is the electrical conductivity of the material.

### C. PROXIMITY EFFECT

A large number of copper coils are bundled inside the motor stator slots, and a magnetic field is generated because

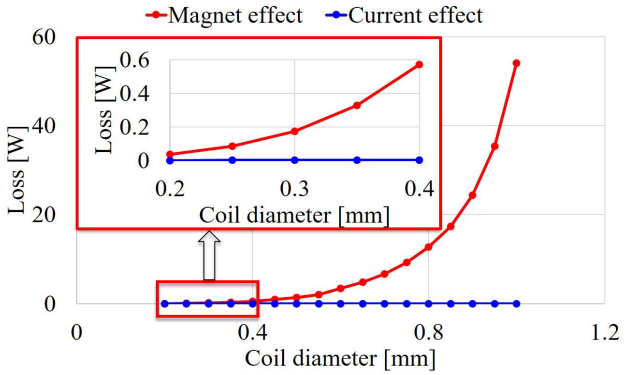



**FIGURE 4.** Separation of AC copper loss components in slotless PMSM according to round coil diameter.

an AC current flows through them. Since these coils are bundled, they are close together, and the magnetic field generated by one coil affects the adjacent coils. At this time, according to Faraday Lenz's law, eddy currents are generated near the adjacent coil in a direction that opposes the main current flow, as shown in Fig. 1 (b). On the opposite side, the eddy currents flow in the same direction as the main current, causing the main current to crowd toward one side. This increases the equivalent resistance of the copper coil and leads to higher copper losses, a phenomenon known as the proximity effect. In addition, in a conventional slotted PMSM, the stator core is present, so most of the changing magnetic field from the rotating permanent magnets flows through the core without significantly affecting the copper coils. However, in a slotless PMSM, since there is no stator core, the magnetic field from the rotating permanent magnets directly links with the copper coils, significantly increasing the proximity effect. To confirm this, the AC copper loss and DC copper loss of the slotless PMSM were separated and analyzed, as shown in Fig. 3 and Fig. 4. Fig. 3. shows the separation of each loss component that makes up the copper loss of the slotless PMSM, divided into DC copper loss and AC copper loss. As shown in (1), the DC copper loss is proportional to the square of the current and the resistance. The AC copper loss can be separated into the AC copper loss caused by the current and the AC copper loss caused by the permanent magnet flux. The loss components shown in Fig. 3 were separated by means of finite element analysis. The DC copper loss can be calculated from the rms current and the DC resistance in (1). The AC copper loss due to armature reaction can be obtained by rotating the machine at the rated speed with only the phase current applied while the remanent flux density of the permanent magnets is set to zero. In addition, the AC copper loss due to the proximity effect produced by the permanent-magnet flux can be obtained from the eddy currents induced in the coils when the machine is rotated at the rated speed without any phase current applied. The analysis results confirm that in the slotless PMSM, the AC copper loss due to current is negligible, while the AC copper loss due to permanent magnet flux accounts for most of it.

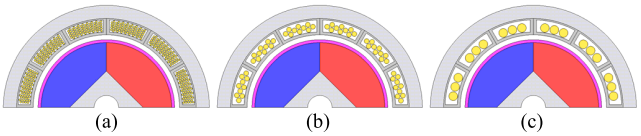



**FIGURE 5.** Geometry of the slotless PMSM to round coil diameter (a) 0.2mm, (b) 0.5mm, (c) 0.9mm.

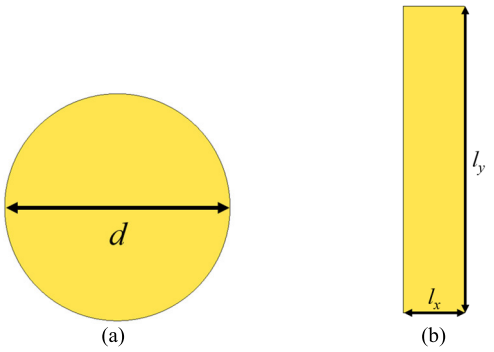



**FIGURE 6.** Conductor geometry of the slotless PMSM (a) round conductor (b) square conductor.

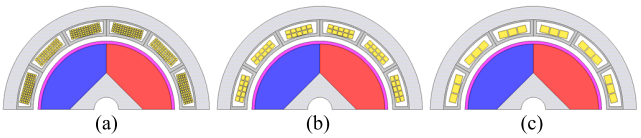



**FIGURE 7.** Geometry of the slotless PMSM to large $l_x$ square coil diameter (a) $l_x$: 0.2mm, (b) $l_x$: 0.5mm, (c) $l_x$: 0.9mm.

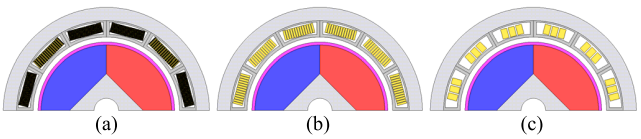



**FIGURE 8.** Geometry of the slotless PMSM to large $l_y$ square coil diameter (a) $l_x$: 0.03mm, (b) $l_x$: 0.2mm, (c) $l_x$: 0.64mm.

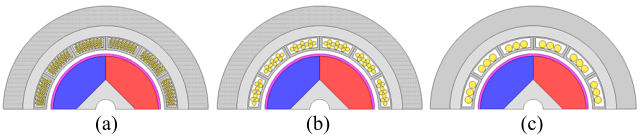



**FIGURE 9.** Geometry of the slotless PMSM with housing according to the round-coil diameter (housing thickness fixed at 2.5 mm): (a) 0.2 mm, (b) 0.5 mm, (c) 0.9 mm.

Fig. 4. shows the AC copper loss as a function of the round coil size in the slotless PMSM. It can be seen that as the round coil size increases, the loss increases sharply in proportion to the square of the diameter, as shown in (4). This also confirms that the AC copper loss due to the permanent magnet flux accounts for most of the total loss. The proximity effect can be expressed as shown in (4), which indicates that the AC copper loss due to the proximity effect is proportional to the square of the flux density, the square of the frequency, and

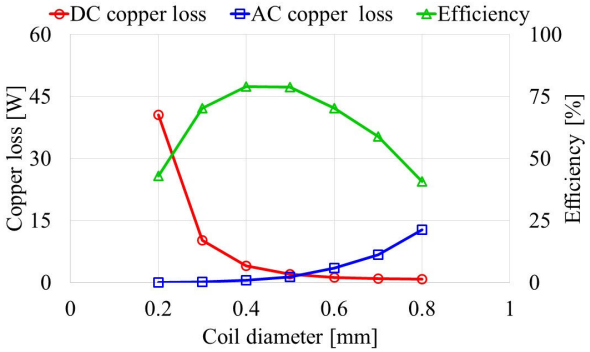



**FIGURE 10.** Efficiency and copper loss characteristics according to round coil diameter in slotless PMSM.

the square of the coil diameter [14], [16], [28], [29]. To reduce AC copper loss due to the proximity effect, practical methods include reducing the coil diameter or lowering the operating speed. Furthermore, since the flux density directly linked to the coils is higher in slotless PMSMs than in slotted PMSMs, the impact of the AC copper loss due to the proximity effect is very large. Therefore, it is confirmed that reducing the coil diameter is critical to mitigating this loss.

$$P_{circ} = \frac{B_m^2 \cdot \omega^2 \cdot d^2}{32 \cdot \rho} \tag{4}$$

where, $P_{circ}$ is the eddy current loss per unit volume of round coil, $B_m$ is the peak magnetic flux density at the conductor location, $\omega$ is the angular frequency, $d$ is the conductor diameter, $\rho$ is the electrical resistivity of the conductor.

## III. AC COPPER LOSS ANALYSIS IN SLOTLESS PMSM

To analyze AC copper losses, finite element analysis (FEA) is used to investigate the effects of coil shape, size, and housing material on AC copper losses. Therefore, this section describes the analysis conditions and explains the geometry of each model.

### A. GEOMETRY FOR ANALYSIS OF AC COPPER LOSS

This section describes the model geometries used to analyze the AC copper losses of the slotless PMSM. The initial dimensions of the base model were determined by referring to the outer diameter, rated torque, speed, and current of a reference model, and the design was subsequently carried out through parametric analysis based on finite element analysis. First, the geometry of the slotless PMSM is shown in Fig. 2. As illustrated in Fig. 2, the rotor geometry of the slotless PMSM is identical to that of a conventional slotted surface-mounted PMSM. However, the stator does not have slots; instead, it consists of a stator yoke, coils, and a plastic insulation structure to support the coils. Therefore, it does not suffer from cogging torque like slotted structures. In addition, while the magnetic air gap and mechanical air gap are identical in slotted PMSMs because the slots are made of iron cores, the mechanical and magnetic air gaps are different in slotless PMSMs, as shown in Fig. 2, because the stator slot area

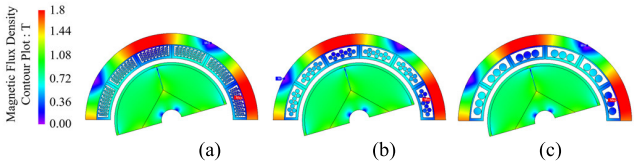



**FIGURE 11.** Magnetic flux density in slotless PMSM according to round coil diameter (a) 0.2mm, (b) 0.5mm, (c) 0.9mm.

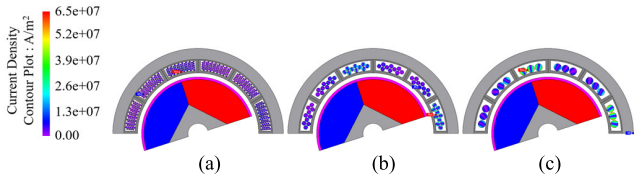



**FIGURE 12.** Current density in slotless PMSM according to round coil diameter (a) 0.2mm, (b) 0.5mm, (c) 0.9mm.

is made of plastic insulation instead of iron. Consequently, the slotless PMSM has a larger magnetic air gap than the slotted PMSM. Fig. 5. shows the slotless PMSM geometries used to analyze AC copper loss as a function of the round-coil diameter. Specifically, (a), (b), and (c) represent coil diameters of 0.2 [mm], 0.5 [mm], and 0.9 [mm], respectively. Additionally, the number of coil turns is selected to maximize the slot fill factor within the plastic insulation structure shown in Fig. 2. Since the slot area is fixed, the number of turns decreases as the coil diameter increases. For square coils, the AC copper loss analysis was conducted using two different models. Fig. 7. shows the model with large $l_x$ coils, where (a) has a width $l_x$ of 0.2 [mm] and a length $l_y$ of 0.16 [mm], (b) has a width $l_x$ of 0.5 [mm] and a length $l_y$ of 0.39 [mm], and (c) has a width $l_x$ of 0.9 [mm] and a length ly of 0.71 [mm]. Fig. 8. shows the model with large $l_y$ coils, where (a) has a width $l_x$ of 0.03 [mm] and a length $l_y$ of 1 [mm], (b) has a width $l_x$ of 0.2 [mm] and a length $l_y$ of 1 [mm], and (c) has a width $l_x$ of 0.64 [mm] and a length $l_y$ of 1 [mm]. Similar to the round coil models, since the slot area is fixed in the square coil models, the number of turns decreases as the width increases. Fig. 9. shows the slotless PMSM models used to analyze Housing AC copper loss as a function of the round coil diameter. Here, (a), (b), and (c) represent coil diameters of 0.2 [mm], 0.5 [mm], and 0.9 [mm], respectively. In this manner, various slotless PMSMs are modeled based on coil shapes, coil diameters, permanent magnet magnetization directions, and housing thicknesses to analyze how each parameter affects AC copper loss in slotless PMSMs via FEA simulations.

### B. CONSTRAINT

This section describes the motor constraints used to accurately analyze AC copper losses as a function of coil diameter, coil shape, permanent magnet magnetization direction, and housing material for the slotless PMSM. Since the speed, torque, and current are fixed, the effects of different variables on AC copper loss can be analyzed at a given output power. First, the constraints for the round coil, based on coil

**TABLE 1. Design variables and specifications of the slotless PMSM models.**

| Symbol | Quantity | Value | | | | | | | | Unit |
|---|---|---|---|---|---|---|---|---|---|---|
| (a) Common specifications (identical for all models) | | | | | | | | | | |
| $S_o$ | stator outer | 21 | | | | | | | | mm |
| $S_y$ | stator yoke | 1.345 | | | | | | | | mm |
| $A_g$ | air gap | 0.5 | | | | | | | | mm |
| $R_o$ | rotor outer | 13.92 | | | | | | | | mm |
| $R_y$ | rotor yoke | 2.51 | | | | | | | | mm |
| $N_p$ | number of pole | 4 | | | | | | | | - |
| $A_{slot}$ | area of slot | 4.72 | | | | | | | | $mm^2$ |
| $a$ | number of parallel | 1 | | | | | | | | - |
| $T$ | torque | 27 | | | | | | | | mNm |
| $S$ | speed | 12900 | | | | | | | | r/min |
| $A$ | current | 1.73 | | | | | | | | $A_{rms}$ |
| $H_t$ | housing thickness | 2.5 | | | | | | | | mm |
| $C_s$ | coil cross section | 0.03 | 0.07 | 0.13 | 0.2 | 0.28 | 0.38 | 0.5 | 0.64 | $mm^2$ |
| (b) Model A : Round coil | | | | | | | | | | |
| $C_d$ | coil diameter | 0.2 | 0.3 | 0.4 | 0.5 | 0.6 | 0.7 | 0.8 | 0.9 | mm |
| $L_{stk}$ | stack length | 4.7 | 10.9 | 20.2 | 37 | 77.4 | 104.6 | 120.7 | 198.2 | mm |
| $N_{ph}$ | total series turns | 144 | 66 | 36 | 20 | 10 | 8 | 8 | 6 | - |
| (c) Model B : Large $l_x$ square coil | | | | | | | | | | |
| $l_x$ | Coil width | 0.2 | 0.3 | 0.4 | 0.5 | 0.6 | 0.7 | 0.8 | 0.9 | mm |
| $l_y$ | Coil length | 0.16 | 0.24 | 0.31 | 0.39 | 0.47 | 0.55 | 0.63 | 0.71 | mm |
| $Lstk$ | Stack length | 5.4 | 10.3 | 16.9 | 36.3 | 38.8 | 105.5 | 172.5 | 244.7 | mm |
| $Nph$ | Total series turns | 130 | 68 | 42 | 20 | 20 | 8 | 6 | 6 | - |
| (d) Model C : Large $l_y$ square coil ($l_y$ fixed :1mm) | | | | | | | | | | |
| $l_x$ | Coil width | 0.03 | 0.07 | 0.13 | 0.2 | 0.28 | 0.38 | 0.5 | 0.64 | mm |
| $L_{stk}$ | Stack length | 3.7 | 8.6 | 15.5 | 27.5 | 40.5 | 54.5 | 82.3 | 162.9 | mm |
| $N_{ph}$ | total series turns | 190 | 82 | 46 | 26 | 18 | 14 | 10 | 6 | - |
| (e) Model D : Housing model (Round coil) | | | | | | | | | | |
| $C_d$ | Coil diameter | 0.2 | 0.3 | 0.4 | 0.5 | 0.6 | 0.7 | 0.8 | 0.9 | mm |
| $L_{stk}$ | Stack length | 5 | 11.2 | 21.4 | 41.6 | 103 | 159 | 199.9 | 586 | mm |
| $N_{ph}$ | total series turns | 144 | 66 | 36 | 20 | 10 | 8 | 8 | 6 | - |

diameter, are shown in Table 1 (a). As shown in Table 1 (b), as the coil diameter increases, the number of turns decreases because the slot area available for the coils is fixed. However, because the current is fixed, fewer turns reduce torque. Therefore, to maintain the same output power, the stack length was increased as the coil diameter increased to investigate the impact on the AC copper loss. Similarly, to examine the effects of the large $l_x$ and $l_y$ square coil diameters, the constraints were set as shown in Table 1 (c), (d). As shown in Table 1 (c), (d). for square coils, since the slot area is fixed, the number of turns decreases, and the stack length increases with coil geometry. In addition, because the AC copper loss in square coils varies significantly depending on whether the coil shape is large $l_x$ square or large $l_y$ square, the effect of the coil geometry was analyzed. To analyze the effect of the housing on the AC copper loss, the constraints when the housing is present, and the coil diameter changes are shown in Table 1 (e).

## IV. AC COPPER LOSS OPTIMIZATION IN SLOTLESS PMSM

Previously, the effects of each slotless PMSM model parameter on output performance were analyzed using FEA to investigate AC copper losses.

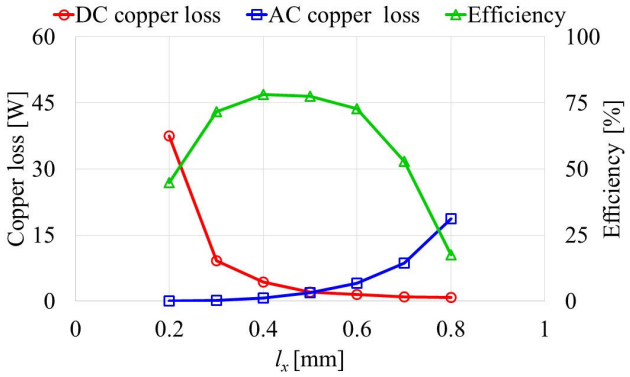



**FIGURE 13.** Efficiency and copper loss characteristics according to large $l_x$ square coil diameter in slotless PMSM.

### A. EFFECT OF ROUND CONDUCTOR SIZE ON AC COPPER LOSS

To analyze the AC copper losses in round coils, modeling was performed for coil diameters ranging from 0.2 [mm] to 0.9 [mm], as shown in Fig. 5. In addition, Fig. 11 and Fig. 12. show the magnetic flux density and Joule loss density for coil sizes of 0.2 [mm], 0.5 [mm], and 0.9 [mm] to compare the AC copper losses of the round coils. The coils were selected to fully occupy the slot area. Since the slot area is fixed, the number of turns decreases as the coil diameter increases. Therefore, to analyze the AC copper losses under the same output power, the stack length was increased when the number of turns decreased, as shown in Table 1, to satisfy the target output specification. At a coil diameter of 0.2 [mm], the number of turns is larger than that at 0.9 [mm]. Consequently, as analyzed from (1) and Fig. 10, the DC copper loss becomes very large. However, because the coil diameter is small, the AC copper loss is extremely small since it is proportional to the square of the coil diameter, as indicated in (4). Conversely, when the coil diameter is 0.9 [mm], the number of turns decreases due to the fixed slot area, so the stack length is increased to maintain the output power. Although the stack length increases, the DC copper loss is small because the number of turns is significantly reduced. On the other hand, the AC copper loss increases sharply with the square of the coil diameter, making it dominant over the DC copper loss. These results indicate that even if the coil diameter is reduced to mitigate AC copper losses, the number of turns increases, thereby significantly increasing DC copper losses and reducing efficiency. On the contrary, if the coil diameter is increased to reduce DC copper losses, the AC copper losses become very large, also leading to a drop in efficiency. Therefore, it is essential to select an optimal coil diameter to minimize both DC and AC copper losses and achieve maximum efficiency in slotless PMSMs. As shown in Fig. 10, the maximum efficiency occurs at a coil diameter of 0.5 [mm] in this model, where both DC and AC copper losses are minimized.

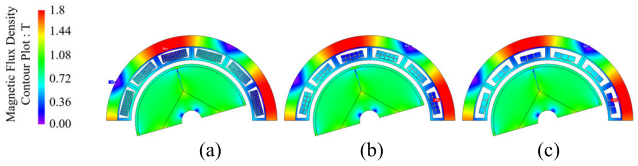



**FIGURE 14.** Magnetic flux density in slotless PMSM according to large $l_x$ square coil diameter (a) 0.2mm, (b) 0.5mm, (c) 0.8mm.

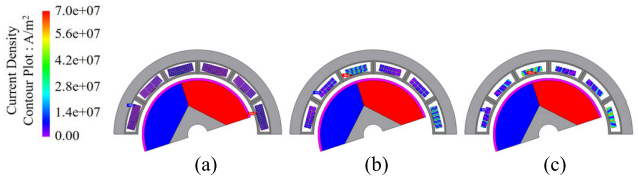



**FIGURE 15.** Current density in slotless PMSM according to large $l_x$ square coil diameter (a) 0.2mm, (b) 0.5mm, (c) 0.8mm.

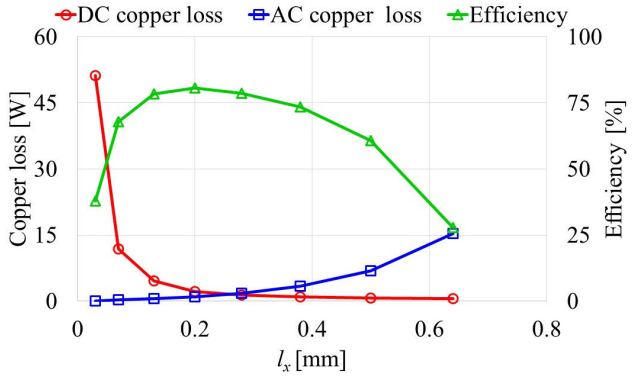



**FIGURE 16.** Efficiency and copper loss characteristics according to large $l_y$ square coil diameter in slotless PMSM.

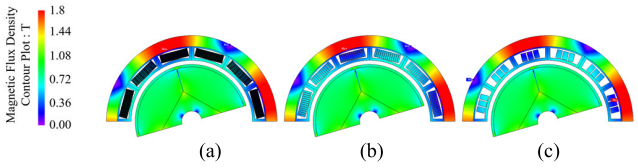



**FIGURE 17.** Magnetic flux density in slotless PMSM according to large $l_y$ square coil diameter (a) 0.03mm, (b) 0.2mm, (c) 0.64mm.

### B. EFFECT OF SQUARE CONDUCTOR GEOMETRY ON PROXIMITY INDUCED AC COPPER LOSS

Unlike round coils, square coils consist of a width $l_x$ and a height ly, as shown in Fig. 6. Therefore, the area linked by the magnetic flux generated by the permanent magnets varies, which changes the AC copper loss depending on $l_x$ and $l_y$. To analyze this effect, two cases are investigated: one where $l_x$ is equal to the diameter of the round coil with the same cross-sectional area, and another where $l_y$ is fixed at 1 [mm] with the same cross-sectional area. For square coils, the AC copper loss due to the proximity effect is derived differently from the conventional equation (4). The AC copper loss caused by the proximity effect in square coils is expressed as shown

in (5) [14], [16], [25], [26]. As indicated in (5), the AC copper loss in square coils is proportional to the square of $l_x$, which is the side perpendicular to and directly linked with the magnetic flux generated by the permanent magnets, as well as the square of the flux density and the square of the frequency. Therefore, to reduce the AC copper loss in square coils, it is critical to lower the motor speed or decrease the length $l_x$.

$$P_{rect} = \frac{B_m^2 \cdot \omega^2 \cdot l_x^2}{24 \cdot \rho} \tag{5}$$

where, $P_{rect}$ is the eddy current loss per unit volume in the square coil, $B_m$ is the peak magnetic flux density at the conductor location, $\omega$ is the angular frequency, $l_x$ is the width of the square coil (perpendicular to the magnetic flux generated by the permanent magnets), $\rho$ is the electrical resistivity of the conductor.

### C. ANALYSIS OF LOSS AND EFFICIENCY CHARACTERISTICS ACCORDING TO SQUARE COIL DIMENSIONS

Fig. 7. shows the designed models as the variable $l_x$ changes from 0.2 [mm] to 0.9 [mm]. At this time, because the cross-sectional area of the square coil must be kept equal to that of the round coil, the value of $l_y$ is dependently determined according to the variation of $l_x$. Therefore, the loss and output characteristics as a function of $l_x$ are analyzed. It can be confirmed that the AC copper loss increases sharply as $l_x$ increases, based on the analysis of the loss and efficiency comparison in Fig. 13, the magnetic flux density in Fig. 14, and the current density in Fig. 15. This is because the AC copper loss of the square coil is proportional to the square of $l_x$, as shown in (5). For DC copper loss, since the slot area is assumed constant and the slot fill factor is maximized, a smaller $l_x$ increases the number of turns, leading to higher DC copper losses. Conversely, as $l_x$ increases, the number of turns decreases, thereby reducing DC copper loss. As a result, the maximum efficiency occurs in the range of 0.4 [mm] to 0.5 [mm], where the AC and DC copper losses cross. This confirms that for square coils, as with round coils, the AC copper loss has a significant impact on the output characteristics. On the other hand, when the variable $l_y$ in Fig. 7. is fixed at 1 [mm], and the cross-sectional area is kept equal to that of the round coil, $l_x$ is dependently determined and becomes very short. Consequently, the area linked by the permanent magnet flux decreases, confirming that the AC copper loss is reduced as predicted by (5). The analysis results show that, as illustrated in Fig. 16, Fig. 17, and Fig. 18, the AC copper loss is lower, and the efficiency is higher compared to the round coil or the models with a large $l_x$. Therefore, when designing square coils, minimizing $l_x$, the length perpendicular to the permanent magnet flux, is an effective way to reduce AC copper losses.

### D. COMPARATIVE ANALYSIS OF PERFORMANCE AND LOSSES FOR ROUND AND SQUARE COIL MODELS

compared and analyzed according to the sizes of the round coils and square coils. Model A represents the round coil model, Model B represents the square coil model with a large $l_x$, and Model C represents the model with a large $l_y$. Fig. 19. compares the efficiency of each model, and Fig. 20.

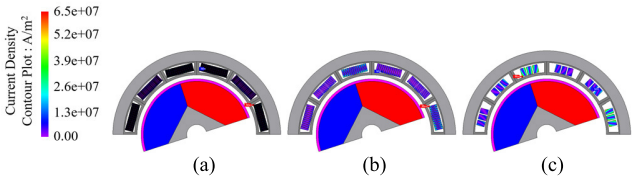



**FIGURE 18.** Current density in slotless PMSM according to large $l_y$ square coil diameter (a) 0.03mm, (b) 0.2mm, (c) 0.64mm.

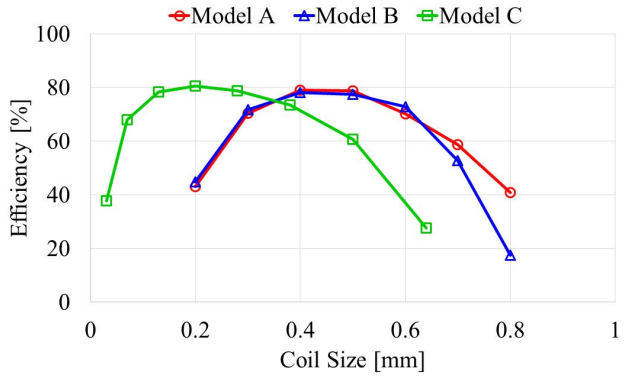



**FIGURE 19.** Efficiency characteristics according to coil shape and size.

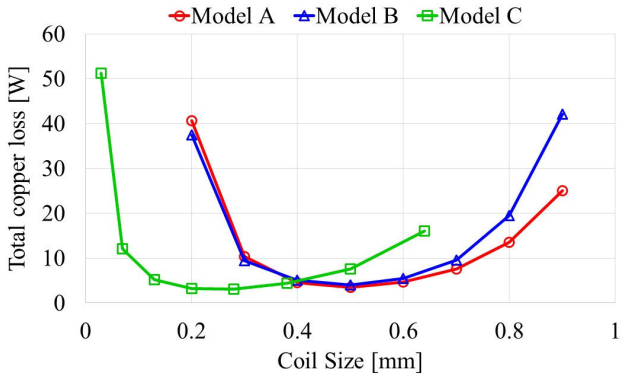



**FIGURE 20.** Copper loss characteristics according to coil shape and size.

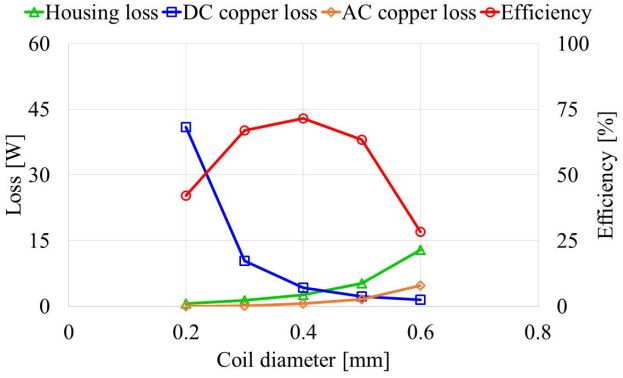



**FIGURE 21.** Efficiency and loss characteristics of a slotless PMSM with housing.

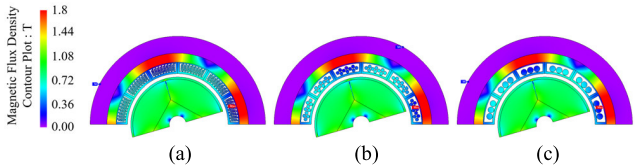



**FIGURE 22.** Magnetic flux density of a slotless PMSM with housing according to round coil diameter (a) 0.2mm, (b) 0.5mm, (c) 0.9mm.

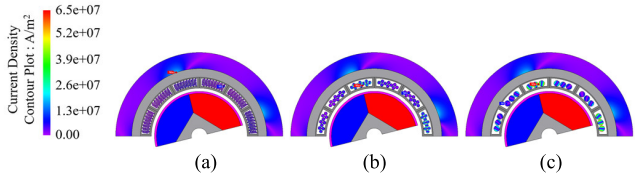



**FIGURE 23.** Current density of a slotless PMSM with housing according to round coil diameter (a) 0.2mm, (b) 0.5mm, (c) 0.9mm.

compares the total copper losses. The analysis results show that when the coil size is small, the efficiency of Model C, which has a large DC copper loss, is the lowest; this is because the AC copper loss is negligible and the DC copper loss is dominant, as shown in (4) and (5). However, as the coil size increases, the AC copper loss increases sharply while the DC copper loss decreases, making the AC copper loss dominant. Therefore, Model C, which has a smaller AC copper loss, exhibits the highest efficiency. These findings confirm that, in slotless PMSMs, the dominant loss component and the optimal efficiency point vary with coil size. Consequently, it is highly important to consider and mitigate AC copper losses when designing slotless PMSMs. Furthermore, unlike round coils, square coils have a fixed minimum manufacturable length. Since the coil sizes at the maximum-efficiency points for Models B and C cannot be manufactured, using round coils with smaller sizes is the most effective approach for slotless PMSMs.

### *E. EFFECT OF HOUSING EDDY CURRENT LOSS ON AC COPPER LOSS AND OUTPUT PERFORMANCE*

Unlike slotted motors, slotless permanent magnet synchronous motors (PMSMs) have only a stator yoke without stator teeth, which causes the magnetic flux to leak into the housing. Therefore, to compare loss characteristics for housing loss in slotless PMSMs, the variation in housing loss with coil diameter in the round-coil model is investigated. Fig. 9. shows the round coil models with diameters ranging from 0.2 [mm] to 0.9 [mm] to examine housing loss, with the housing thickness fixed at 2.5 [mm]. To analyze the housing loss, the output power as a function of coil diameter Fig. 21. the magnetic flux density Fig. 22. and the current density Fig. 23. are investigated. The analysis results confirm that efficiency further decreases with the addition of housing loss. This can be analyzed more clearly by comparing the efficiency and losses with those without the housing loss in Fig. 24. The maximum efficiency without the housing loss is over 78%,

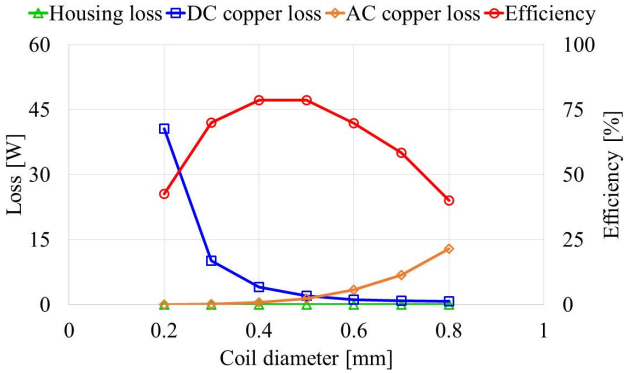



**FIGURE 24.** Efficiency and loss characteristics of a slotless PMSM without housing.

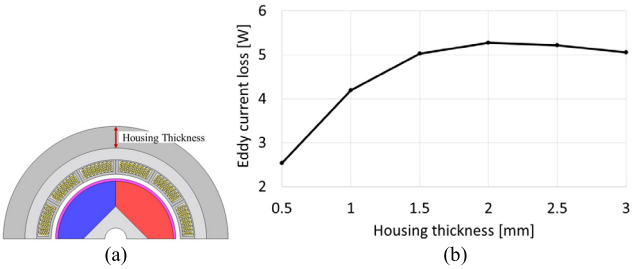



**FIGURE 25.** Eddy current loss of a slotless PMSM with housing according to housing thickness based on a reference model with a round coil diameter of 0.5 mm. (a) housing thickness, (b) analysis results.

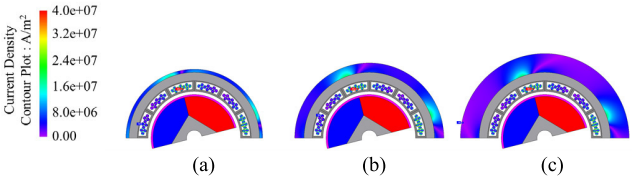



**FIGURE 26.** Current density of a slotless PMSM with housing and round coil coils according to housing thickness based on a reference model with a round coil diameter of 0.5 mm (a) 0.5mm, (b) 1.5mm, (c) 3mm.

but it decreases to approximately 71% when the housing loss is included. In addition, it is confirmed that AC copper loss increases when housing loss is present. This is because the counter torque from the housing eddy-current loss requires a longer stack length to maintain the same output power with the same number of turns and current, thereby increasing AC copper loss. Since minimizing housing loss is critical to improving the output performance of slotless PMSMs, the loss characteristics as a function of housing thickness were analyzed to reduce housing eddy-current losses. Fig. 25(a) shows the model geometry as the housing thickness increases from 0.5 [mm] to 3 [mm], and Fig. 25(b) shows the eddy current loss as the housing thickness increases. It can be seen that the housing eddy-current loss decreases as the housing thickness decreases, because the cross-sectional area available for eddy-current flow is reduced. However, when the housing thickness increases beyond 2 [mm], the total magnetic flux linking the housing decreases due to the counter-magnetic

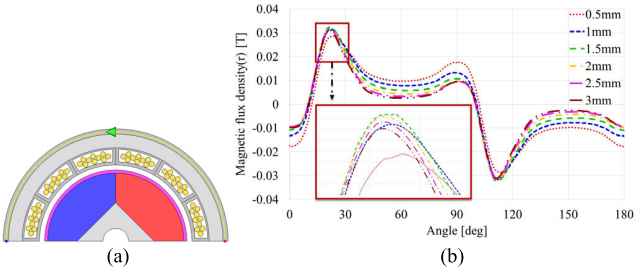



**FIGURE 27.** Radial magnetic flux density of a slotless PMSM with housing according to housing thickness (a) measurement position, (b) radial magnetic flux density according to thickness.

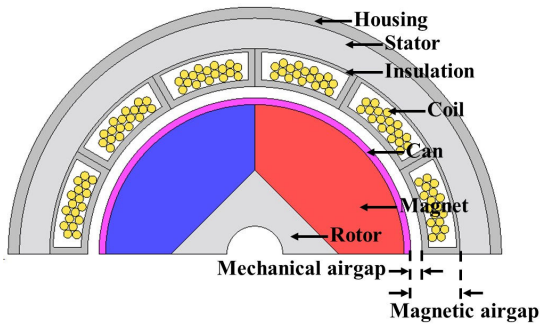



**FIGURE 28.** Structure of final model slotless PMSM.

**TABLE 2.** Specification and constraints for slotless PMSM.

| Content | Slotless PMSM | Unit |
|---|---|---|
| rated power | 35.12 | W |
| rated speed | 12900 | rpm |
| rated torque | 26 | mNm |
| input current | 1.68 | $A_{rms}$ |
| stator outer | 21 | mm |
| stack length | 22 | mm |
| number of poles | 4 | - |
| number of slots | 12 | - |
| airgap length | 0.5 | mm |
| thickness of magnet | 4 | mm |
| thickness of housing | 1 | mm |
| total series turn | 36 | - |
| number of parallel branches | 1 | - |
| area of slot | 4.72 | $mm^2$ |
| diameter of coil | 0.37 | mm |
| material of housing | aluminum | - |
| material of core | 35pn230 | - |
| material of magnet | N45UH | - |

field generated by the housing's eddy currents, thereby reducing the loss. This is verified by the housing current density shown in Fig. 26, which indicates that the loss occurs only on the inner side of the housing, and almost no current is generated further inside as the housing becomes thicker. Fig. 27 (a) shows the magnetic flux density measurement points in the r direction to analyze the reduction in loss when the housing thickness exceeds 2 [mm]. As shown in Fig. 27(b), the magnetic flux density flowing through the housing gradually decreases as the housing thickness exceeds 2 [mm]. Therefore, it can be concluded that in slotless PMSMs, reducing AC copper loss in the coils and mitigating eddy-current loss caused by flux flowing through the housing are highly critical for improving output performance. However, reducing the housing thickness involves a practical trade-off: although a thinner housing lowers the eddy-current loss, it also reduces the mechanical rigidity that protects and supports the stator and decreases the surface area available for heat dissipation. Therefore, in a real design the minimum housing thickness must be determined by balancing the eddy-current loss against the required structural strength and thermal performance, rather than by minimizing the loss alone.

### *F. COMPREHENSIVE DESIGN RESULTS AND ELECTROMAGNETIC CHARACTERISTICS OF THE FINAL MODEL*

Unlike conventional slotted permanent magnet synchronous motors (PMSMs), slotless PMSMs require careful consideration of AC copper losses. To reduce AC copper losses, parameters such as coil shape, coil size, housing material, and thickness must be considered. Therefore, the specifications and geometry of the final model, designed with these design variables, are presented in Table 2 and Fig. 28. In the final model, the stator core is made of 35PN230 electrical steel, the permanent magnets are N45UH NdFeB magnets, and the housing is made of aluminum, as summarized in Table 2. To increase output power while minimizing AC copper losses, a square coil with a short width $l_x$ and a long height $l_y$ should be used. However, because square shapes are difficult to manufacture, a round coil with a small coil diameter was used to effectively reduce the AC copper losses. A smaller coil diameter was selected because AC copper loss increases sharply with increasing coil diameter, thereby reducing output performance. In addition, unlike slotted PMSMs, slotless PMSMs lack a stator tooth structure, causing flux from the stator back yoke to leak into the housing and increasing housing eddy-current losses. Therefore, using a non-conductive material for the housing is suitable for slotless PMSMs. However, since it is difficult to find a non-conductive material that provides both good heat dissipation and sufficient structural rigidity, aluminum must be used in practice. Nevertheless, because aluminum is a conductor, when the back yoke flux leaks into the aluminum housing, eddy-current losses occur, reducing the output power. Consequently, the housing thickness was designed to be as thin as possible to reduce eddy-current losses while improving output performance. A housing thickness of 1[mm] was selected as the final design. By considering these losses in the slotless PMSM, the final designed model achieved a torque of 26 [mNm], a speed of 12900 [r/min], and an efficiency of 80.22 [%]. Fig. 29. shows the magnetic flux density of the final designed slotless PMSM, while Fig. 30 (a) and (b)

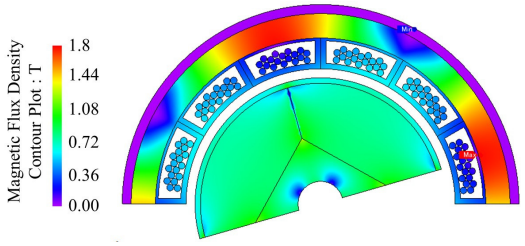



**FIGURE 29.** Magnetic flux density of the final model of the slotless PMSM.

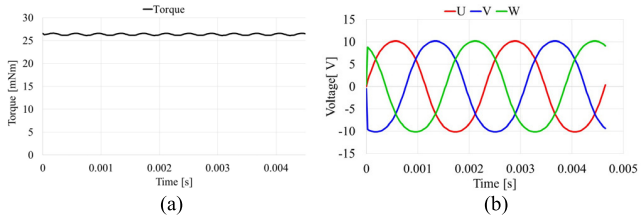



**FIGURE 30.** Torque and load voltage of the final model of the slotless PMSM (a) load torque, (b) load voltage.

present the torque and load voltage, respectively. Fig. 31. illustrates the loss breakdown of the final slotless PMSM model. The total loss of the final model is 7.51[W], consisting of DC copper loss 4.61[W], housing loss 1.36[W], iron loss 1.06[W], and AC copper loss 0.48[W]. The housing loss corresponds to 18.11[%] of the total loss and 3.87[%] of the rated output power 35.12[W], confirming that although it is not the dominant loss component, it remains a non-negligible contribution that must be considered in the design of slotless PMSMs.

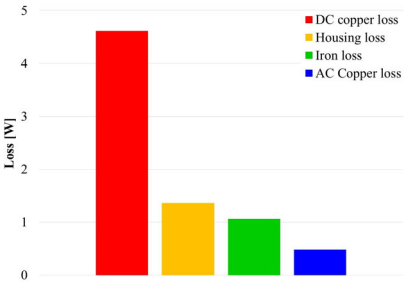



**FIGURE 31.** Loss analysis of the final model of the slotless PMSM at round coil 0.37mm.

## V. FINAL ELECTROMAGNETIC DESIGN AND MANUFACTURE OF THE SLOTLESS PMSM

In this section, tests were conducted to verify the electromagnetic design results and the actual fabrication of the slotless permanent magnet synchronous motor (PMSM).

### A. STRUCTURAL DESIGN AND MANUFACTURING ADVANTAGES OF THE NOVEL BLOCK COIL STATOR

Conventional winding methods for slotless PMSMs cannot be manufactured due to exclusive patents held by advanced global companies. Therefore, in this paper, a novel winding method that completely breaks away from conventional slotless PMSM winding techniques was researched to fabricate the slotless PMSM. Fig. 32. shows the 3D modeling of the new slotless PMSM. The stator consists of coils, a plastic injection-molded structure, and a back yoke with a block-like assembly. As described, the winding method applied to the slotless PMSM in this study is a novel technique that completely bypasses the patented conventional methods. Because the stator can be constructed by assembling the coils like blocks, it offers distinct advantages in manufacturing and maintenance. Furthermore, because the coils are assembled and fixed to one another like blocks, the structure is robust. Accordingly, Fig. 33 (a) shows a single block coil unit, (b) shows the actually assembled block coil stator, and (c) presents the fabricated motor unit integrating the block coils.

### B. EXPERIMENTAL TESTING AND PERFORMANCE VERIFICATION OF THE MANUFACTURED SLOTLESS PMSM

To verify the electromagnetic design results, the slotless PMSM was manufactured and tested. Direct experimental separation of AC and DC copper losses is challenging in practice. This limitation is common to all studies on AC copper losses in PMSMs [3], [4], [5], [14], which similarly

**TABLE 3.** Electromagnetic design and experimental results of slotless pmsm.

| Content | Analysis | Test | Unit |
|---|---|---|---|
| load torque | 26 | 26.02 | mNm |
| speed | 12900 | 12858 | r/min |
| no load voltage@ 1000r/min | 0.623 | 0.623 | $V_{rms}$ |
| fundamental current | 1.68 | 1.73 | $A_{rms}$ |
| Current THD | - | 37.4 | % |
| dc voltage | 24 | 24 | V |
| output power | 35 | 35 | W |
| Efficiency | 80.22 | 79.1 | - |

rely on FEA-based loss decomposition. The validity of the FEA model used for loss separation is instead confirmed indirectly through close agreement between simulated and measured back-EMF, load torque, and overall efficiency, all within 2% error. Table 3 compares the electromagnetic design and experimental data, verifying the accuracy of the design results. First, the no-load back electromotive force (EMF) of the slotless PMSM was measured to validate the performance. The test setup is shown in Fig. 34. The slotless PMSM was coupled to an external driving motor via a shaft coupling and rotated at 1000 [r/min]. The measurement results were captured using an oscilloscope. Fig. 35. compares the simulated and measured back-EMF waveforms, showing negligible discrepancy between the design and experimental results. Fig. 36. illustrates the load test environment. The fabricated model was designed as a slotless PMSM with a sinusoidal back-EMF. However, because the outer diameter of the model was too small for a Hall sensor to be attached, it was driven by a sensorless square-wave controller; as shown in Fig. 37, a square-wave current flows, which is the reason why the fundamental current differs from the rated current. The motor test was conducted at the

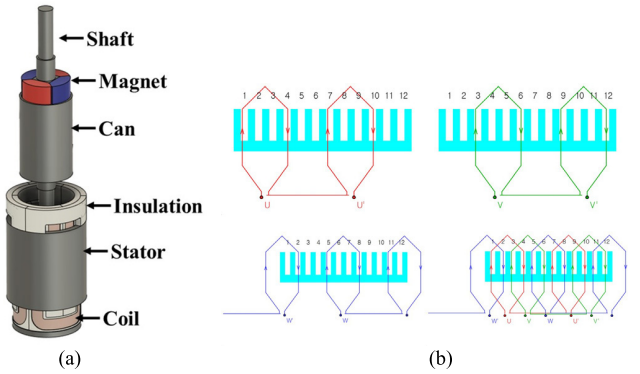



**FIGURE 32.** Final manufactured model of the slotless PMSM (a) 3D Model (b) Winding.

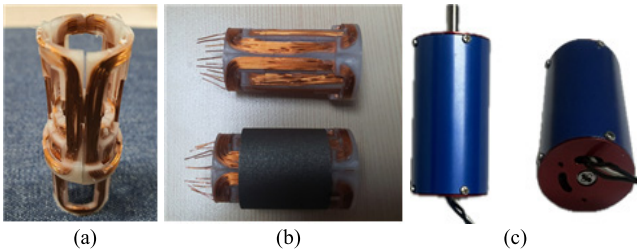



**FIGURE 33.** Configuration of the final manufactured slotless PMSM model (a) block coil geometry, (b) stator, (c) assembled block coil slotless motor.

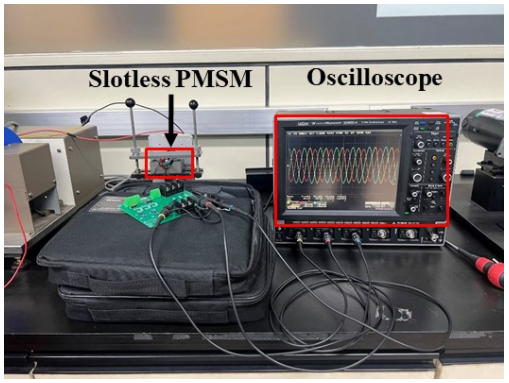



**FIGURE 34.** No load back EMF measurement test environment of the manufactured slotless PMSM.

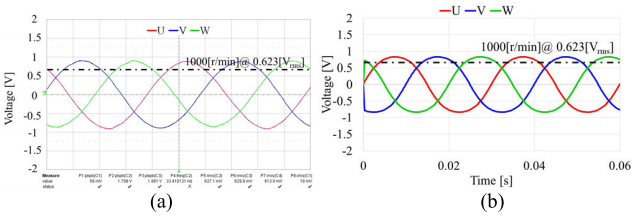



**FIGURE 35.** Comparison of measured no load back EMF data and design results of the manufactured slotless PMSM (a) measured data, (b) design data.

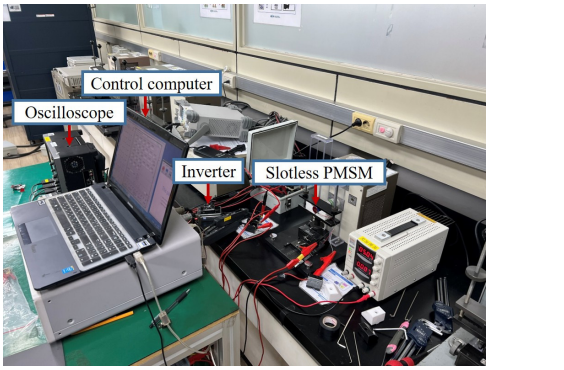



**FIGURE 36.** Load test environment of the manufactured slotless PMSM.

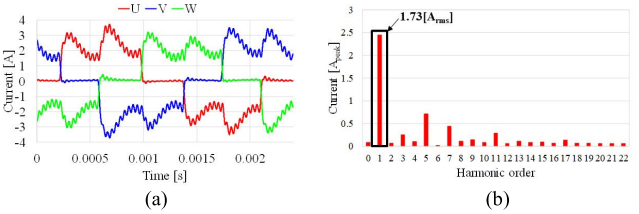



**FIGURE 37.** Measured current and fast fourier transform results of the manufactured slotless PMSM (a) Measured current, (b) FFT result.

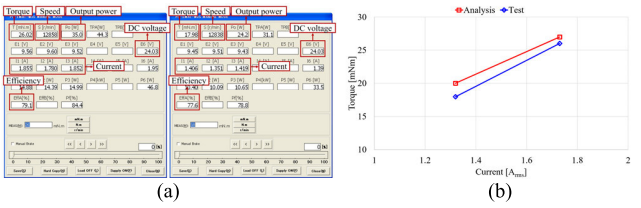



**FIGURE 38.** Comparison of measured load data and design results of the manufactured slotless PMSM (a) Test result, (b) Test torque data.

Korea Electronics Technology Institute (KETI). The motor output was measured using a SUGAWARA TB-1ks torque detector, and the input quantities such as the motor current and voltage were measured using a YOKOGAWA WT1800 power analyzer. The measurement was performed precisely through calibration of the sensors used for the efficiency measurement. Comparing the test results, the designed electromagnetic efficiency is 80.22 [%], while the measured efficiency is 79.1 [%], resulting in a difference of approximately 1 [%p]. In the electromagnetic design, the phase current was assumed to be an ideal sine wave; however, during the actual test, the motor was driven by a square-wave current. The resulting current harmonics increased the actual measured current, leading to the observed reduction in efficiency. To verify this, the current waveform was measured with an oscilloscope, as shown in Fig. 37 (a). An FFT analysis was performed on the raw data, as shown in Fig. 37(b). The analysis shows that the magnitude of the fundamental current is 1.73 [$A_{rms}$], which differs from the design current by approximately 2 [%]. Consequently, because the errors in both the no-load back EMF and the load test efficiency measurements are under 2 [%], the validity of the electromagnetic design results is successfully verified.

## VI. CONCLUSION

In this paper, a slotless permanent magnet synchronous motor (PMSM) was designed using a novel winding method that completely breaks away from the exclusive patented structures that have limited conventional slotless motor research. Unlike slotted PMSMs, slotless PMSMs do not have a stator teeth structure, resulting in zero cogging torque. Furthermore, because they lack a slot-opening structure, spatial harmonics are eliminated, yielding low torque ripple, making them highly suitable for high-precision applications. However, because there are no stator teeth, the permanent magnet flux directly links with the coils, generating a new loss component, AC copper loss, in addition to the conventional DC copper loss. Therefore, to achieve a high-efficiency design for the slotless PMSM, the methods for mitigating AC copper losses were analyzed. The AC copper loss is proportional to the square of the conductor dimension perpendicular to the permanent magnet flux link direction. Consequently, for round coils, the loss is proportional to the square of the coil diameter, whereas for square coils, a square geometry with a short width $l_x$ and a long height $l_y$ is found to be effective in reducing AC copper losses. In addition, because slotless PMSMs lack teeth, a portion of the permanent magnet flux leaks into the housing through the stator yoke. It was confirmed that this leakage flux induces eddy-current losses in the housing, thereby degrading the output performance. To minimize these housing eddy-current losses, an analysis was conducted as a function of housing thickness, confirming that a thinner housing reduces the losses. As described, to mitigate AC copper losses, it is critical to reduce the conductor size and decrease the housing thickness. Based on this analysis, a high-efficiency slotless PMSM was designed by selecting an optimal coil diameter to minimize both AC and DC copper losses, and an optimal thickness to minimize housing eddy-current losses. At this time, the housing thickness was selected as 1 [mm] considering manufacturability. Regarding the coil geometry, because there is a practical limit to the minimum manufacturable $l_x$ for square coils, a small-diameter round coil was used to reduce AC copper loss. The slotless PMSM designed through this analysis was fabricated, and the design results were verified through experimental testing. Finally, the validity of the design was successfully demonstrated with an error rate within 2[%] compared to the simulated efficiency. This study confirms that mitigating AC copper losses is critical to achieving high efficiency in slotless PMSMs.

## REFERENCES


[1] T. R. He, Z. Q. Zhu, F. Xu, H. Bin, D. Wu, L. M. Gong, and J. T. Chen, "Comparative study of 6-slot/2-pole high-speed permanent magnet motors with different winding configurations," *IEEE Trans. Ind. Appl.*, vol. 57, no. 6, pp. 5864–5875, Nov. 2021.

[2] A. S. Abdel-Khalik, S. Ahmed, and A. M. Massoud, "Effect of multilayer windings with different stator winding connections on interior PM machines for EV applications," *IEEE Trans. Magn.*, vol. 52, no. 2, pp. 1–7, Feb. 2016.

[3] K. Liu, X. Fu, M. Lin, and L. Tai, "AC copper losses analysis of the ironless brushless DC motor used in a flywheel energy storage system," *IEEE Trans. Appl. Supercond.*, vol. 26, no. 7, pp. 1–5, Oct. 2016.

[4] H. Hämäläinen, J. Pyrhönen, and J. Nerg, "AC resistance factor in one-layer form-wound winding used in rotating electrical machines," *IEEE Trans. Magn.*, vol. 49, no. 6, pp. 2967–2973, Jun. 2013.

[5] R. Wrobel, D. E. Salt, A. Griffo, N. Simpson, and P. H. Mellor, "Derivation and scaling of AC copper loss in thermal modeling of electrical machines," *IEEE Trans. Ind. Electron.*, vol. 61, no. 8, pp. 4412–4420, Aug. 2014.

[6] J.-M. Seo, J.-H. Kim, I.-S. Jung, and H.-K. Jung, "Design and analysis of slotless brushless DC motor," *IEEE Trans. Ind. Appl.*, vol. 47, no. 2, pp. 730–735, Mar. 2011.

[7] A.-T. Phung, G. Meunier, O. Chadebec, X. Margueron, and J.-P. Keradec, "High-frequency proximity losses determination for rectangular cross-section conductors," *IEEE Trans. Magn.*, vol. 43, no. 4, pp. 1213–1216, Apr. 2007.

[8] Y. Wu, Z. Zhang, D. Chen, and S. Jin, "Investigation and comparison of different calculation methods for AC copper loss of flat copper wire in axial flux permanent magnet motor," *IEEE Trans. Energy Convers.*, vol. 39, no. 1, pp. 169–181, Mar. 2024.

[9] P. Mellor, R. Wrobel, and N. McNeill, "Investigation of proximity losses in a high speed brushless permanent magnet motor," in *Proc. Conf. Rec. IEEE Ind. Appl. Conf. 41st IAS Annu. Meeting*, vol. 3, Tampa, FL, USA, Oct. 2006, pp. 1514–1518.

[10] S. Dai, J. Yang, Z. Wang, J. Yu, and S. Huang, "Investigation on the influence of eccentricity on the AC copper loss of high-speed slotless permanent magnet motor," *IEEE Trans. Magn.*, vol. 59, no. 11, pp. 1–6, Nov. 2023.

[11] J. Liu, X. Fan, D. Li, R. Qu, and H. Fang, "Minimization of AC copper loss in permanent magnet machines by transposed coil connection," *IEEE Trans. Ind. Appl.*, vol. 57, no. 3, pp. 2460–2470, May 2021.

[12] T. Mizuno, S. Enoki, T. Asahina, T. Suzuki, M. Noda, and H. Shinagawa, "Reduction of proximity effect in coil using magnetoplated wire," *IEEE Trans. Magn.*, vol. 43, no. 6, pp. 2654–2656, Jun. 2007.

[13] X. Chen, H. Fang, X. Fan, H. Hu, D. Li, and R. Qu, "Suppression of winding AC copper loss in high-speed electrical machines by a practical transposition technique," *IEEE Trans. Ind. Appl.*, vol. 58, no. 6, pp. 7121–7130, Nov. 2022.

[14] W. Yu, W. Hua, Z. Zhang, Z. Wu, P. Wang, and W. Xia, "Comparative analysis of AC copper loss with round copper wire and flat copper wire of high-speed stator-PM flux-switching machine," *IEEE Trans. Ind. Appl.*, vol. 58, no. 6, pp. 7131–7142, Nov. 2022.

[15] A. W. Bandarkar, M. K. M. B. Azam, and Y. Sozer, "Comparative performance analysis of slotted and slotless dual-stator and single-rotor axial-flux permanent magnet motor for integrated motor-compressor system," *IEEE Trans. Ind. Appl.*, vol. 61, no. 3, pp. 4234–4245, May 2025.

[16] J. Zhao, W. He, W. Fu, Y. Ding, and Y. Guo, "Comparative studies on performances of slotted and slotless high-speed PMBLDC motors," *IEEE Access*, vol. 12, pp. 13431–13441, 2024.

[17] D. Lee, T. Balachandran, S. Sirimanna, N. Salk, A. Yoon, P. Xiao, J. Macks, Y. Yu, S. Lin, J. Schuh, P. Powell, and K. S. Haran, "Detailed design and prototyping of a high power density slotless PMSM," *IEEE Trans. Ind. Appl.*, vol. 59, no. 2, pp. 1719–1727, Mar. 2023.

[18] B. Hannon, P. Sergeant, and L. Dupré, "Evaluation of the rotor eddy-current losses in high-speed PMSMs with a shielding cylinder for different stator sources," *IEEE Trans. Magn.*, vol. 55, no. 3, pp. 1–10, Mar. 2019.

[19] J. Yang, S. Dai, Z. Wang, Q. Li, J. Yu, J. Wang, and S. Huang, "Influence of rotor eccentricity on electromagnetic performance of rotational symmetrical slotless PM brushless motor," *IEEE Trans. Transport. Electrific.*, vol. 10, no. 2, pp. 3888–3901, Jun. 2024.

[20] Y.-S. Lee, I.-S. Jang, I.-J. Yang, K.-S. Kim, and W.-H. Kim, "Study on the slotless PM motor design process considering high speed," *IEEE Trans. Magn.*, vol. 60, no. 9, pp. 1–4, Sep. 2024.

[21] B. Dehez, F. Baudart, M. Markovic, and Y. Perriard, "Theoretical and experimental investigation of flex-PCB air-gap windings in slotless BLDC machines," *IEEE Trans. Ind. Appl.*, vol. 50, no. 5, pp. 3153–3160, Sep. 2014.

[22] W. Cheng, G. Cao, Z. Deng, L. Xiao, and M. Li, "Torque comparison between slotless and slotted ultra-high-speed AFPM motors using analytical method," *IEEE Trans. Magn.*, vol. 58, no. 2, pp. 1–5, Feb. 2022.

[23] Z. Yang and S. Wang, "Vibration characteristics of slotless rotating armature permanent magnet motors," in *Proc. Int. Conf. Electr. Mach. (ICEM)*, Valencia, Spain, Sep. 2022, pp. 2022–2026.

[24] X. Sun, N. Xu, and M. Yao, "Sequential subspace optimization design of a dual three-phase permanent magnet synchronous hub motor based on NSGA III," *IEEE Trans. Transport. Electrific.*, vol. 9, no. 1, pp. 622–630, Mar. 2023.

[25] N. Xu, N. Li, X. Sun, Y. Wang, and B. Wan, "Robust multi-objective optimisation of an axial-radial flux hybrid excitation permanent magnet synchronous motors based on improved sequential Taguchi method," *IET Electr. Power Appl.*, vol. 19, no. 1, Jan. 2025.
[26] N. Xu, X. Sun, and C. H. T. Lee, "Hierarchical multiobjective optimization of spoke-type axial-flux PMSMs using transfer learning and improved grey wolf algorithm," *IEEE Trans. Ind. Electron.*, vol. 73, no. 5, pp. 6780–6791, May 2026.
[27] H.-C. Liu and J. Lee, "Optimum design of an IE4 line-start synchronous reluctance motor considering manufacturing process loss effect," *IEEE Trans. Ind. Electron.*, vol. 65, no. 4, pp. 3104–3114, Apr. 2018.
[28] T. E. Hajji, S. Hlioui, F. Louf, M. Gabsi, A. Belahcen, G. Mermaz-Rollet, and M. Belhadi, "AC losses in windings: Review and comparison of models with application in electric machines," *IEEE Access*, vol. 12, pp. 1552–1569, 2024.
[29] C. R. Sullivan, "Optimal choice for number of strands in a litz-wire transformer winding," *IEEE Trans. Power Electron.*, vol. 14, no. 2, pp. 283–291, Mar. 1999.



**HYEONBIN HONG** received the M.S. degree in electrical engineering from Hanyang University, Seoul, South Korea, in 2022. He is currently pursuing the Ph.D. degree with the Department of Electrical Engineering, Hanyang University. His research interests include the design, analysis, and control of electrical machines for mechanical and electrical systems. He is particularly interested in applications for electric and hybrid vehicles, industrial electric motors, and precision drive motors.



**HEEWON KOO** received the B.S. degree in electrical engineering from Donga University, Busan, South Korea, in 2022. She is currently pursuing the Ph.D. degree with the Department of Electrical Engineering, Hanyang University, Seoul, South Korea. Her research interests include the design and analysis of electric motors and generators, wireless power transfer systems, and high-efficiency electrical machines for electric vehicle applications.



**CHAEWON JO** received the B.S. degree in electrical engineering from Hongik University, Sejong, South Korea, in 2022. She is currently pursuing the Ph.D. degree with the Department of Electrical Engineering, Hanyang University, Seoul, South Korea. Her research interests include the design and analysis of electrical machines, which are applied in mechanical and electrical systems.



**CHANWOO SON** received the B.S. degree in electrical engineering from Soonchunhyang University, Cheonan, South Korea, in 2021. He is currently pursuing the Ph.D. degree with the Department of Electrical Engineering, Hanyang University, Seoul, South Korea. His research interests include the electrical machine drives and advanced control dual inverter systems.



**JU LEE** (Senior Member, IEEE) received the M.S. degree from Hanyang University, Seoul, South Korea, in 1988, and the Ph.D. degree in electrical engineering from Kyusyu University, Japan, in 1997. In 1997, he joined Hanyang University, where he is currently a Professor with the Department of Electrical and Bio-Engineering. His main research interests include electric machinery and its drives, electro-magnetic field analysis, transportation systems, such as hybrid electric vehicles and railway propulsion systems.